Chapter Two

Photonic crystal fiber

2.1 Introduction

The concept of photonic crystals is founded on an analogy with crystalline solids which are composed of a periodic array of atoms or molecules that can modeled as a periodic potential (Joannopoulos, Meade and Winn 1995). Photonic crystals are formed by arranging dielectric materials in a periodic array or lattice spacing on the order of the light wavelength. Photonic crystals are formed in one, two or three dimensions as shown in figure (2.1):
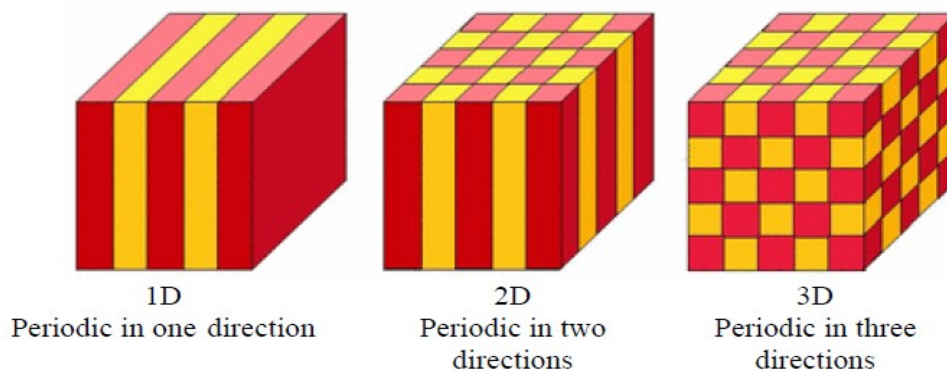

Figure (2.1): One, two, and three dimensional photonic crystal, different colors represent materials with different dielectric constants (Reichenbach 2007).

Photonic Crystal fibers (PCFs) are called sometime microstructured fibers or holy fibers, are the new ways provided to control and guide lights, not obtainable in conventional optical fibers. Proposed for the first time in early 90's, recently PCFs are used in the scientific researches starting in the telecommunication field and then touching metrology, spectroscopy, microscopy, astronomy, biology and sensing (Poli, Cucinotta, and Selleri, 2007).

Nowadays photonic crystal fibers (PCFs) are of much attention all around the world. It consists of central defect region surrounded by multiple air-holes, which run along entire fiber length. Main difference between a PCF and the conventional one is the index profile of core/cladding.PCF can offer more flexibility than conventional fibers in design of optical properties such as birefringence, dispersion and confinement loss. PCF with low and flattened dispersion are useful for improving optical fiber communication capabilities. It has achieved increased attention because of its novel optical characteristics (Amir et al 2013, Oh, K. et al 2005, Feng et al 2003, Saitoh et al. 2010). An important feature of PCF is that it can be made of a single material, in contrast to all other types of optical fibers, which are manufactured with two or more materials (Al Falah, 2009). The design of PCFs is very flexible. There are several parameters to manipulate: lattice pitch, air hole shape and diameter, refractive index of the glass, and type of lattice. Freedom of design allows one to obtain endlessly single mode fibers, which are single mode in all optical range and a cut-off wavelength does not exist (Buczynski, 2004).

Standard (step index) optical fibers guide light by total internal reflection, which operates only if the core has a higher refractive index than the encircling cladding. Rays of light in the core, striking the interface with the cladding, are completely reflected. The wave nature of light dictates that guidance occurs only at certain angles, i.e., that only a small number of discrete "modes" can form. If only one mode exists, the fiber is known as single mode (Russell, 2003). In 1991 Philip Russell emerged idea that the light could trapped a hollow fiber core by creating a periodic wavelength – scale lattice of microscopic holes in cladding glass (Photonic Crystal). The basic principle is the same which is the origin of the color in butterfly wings and

peacock feathers, that is all wavelength-scale periodic structures exhibit ranges of angle and color, stop bands, where incident light is strongly reflected (Poli, Cucinotta, and Selleri, 2007, Russell, 2003). In 1995 the first fiber with photonic crystal was reported by Russell and his colleagues, this fiber are manufactured with a periodic arrangement of low-index material in a background with higher refractive index. The background material in PCFs is usually undoped silica and the low-index region is typically provided by air-holes running along their entire length. The core of this fiber is solid core as shown in figure (2.2).
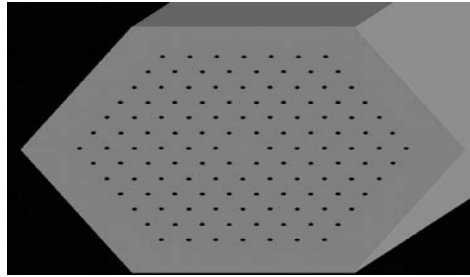

Figure (2.2): shows the cross section of the first solid core photonic crystal fiber (Poli, Cucinotta, and Selleri, 2007).

In 1999 the first hollow core photonic crystal fiber was reported by Russell and his coworkers as shown in figure (2.3).
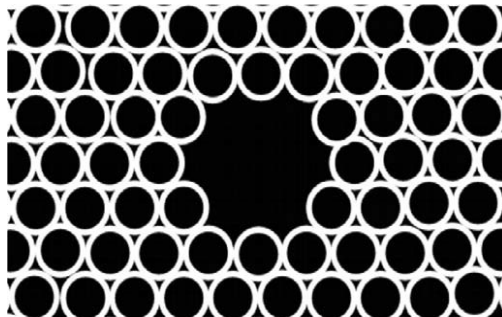

Figure (2.3): Schematic of the cross-section of the first hollow-core PCF (Poli, Cucinotta, and Selleri, 2007).

PCFs have a periodic array of microholes that run along the entire fiber length. They typically have two kinds of cross sections: The first type is an air–silica cladding surrounding a solid silica core(solid – core photonic crystal fibers)

and the second type an air–silica cladding surrounding a hollow core(hollow core photonic crystal fibers)or (HC-PCFs). The light-guiding mechanism of the former is provided by means of a modified total internal reflection (index guiding), while the light-guiding mechanism of the latter is based on the photonic band gap effect (PBG guiding) (Roberts et al. 2006). The number, size, shape, and the separation between the air-holes as well as the air-hole arrangement are what confer PCFs unique guiding mechanism and modal properties. This gives PCF many unique properties such as single mode operation over a wide wavelength range, very large mode area, and unusual dispersion. Because of their freedom in design and novel wave-guiding properties, PCFs have been used for a number of novel fiber-optic devices and fiber-sensing applications that are difficult to be realized by the use of conventional fibers (Massaro, 2012).

2.2 Guiding Mechanism

The guiding mechanism in the photonic crystal fibers depend on the core and cladding refractive index which introduce by the propagation constant β. The highest β value that can exist in an infinite homogeneous medium with refractive index n is $\beta = n k_0$, k_0 being the free-space propagation constant. All the smaller values of β are allowed. A two-dimensional photonic crystal, like any other material, is characterized by a maximum value of β which can propagate. This β value defines the effective refractive index of the material (Poli, Cucinotta, and Selleri, 2007).There are two guiding mechanisms in PCFs:

2.2.1 Modified Total Internal Reflection (MTIR)

It is possible to use a two-dimensional photonic crystal as a fiber cladding, by choosing a core material with a higher refractive index than the cladding

effective index. An example of this kind of structures is the PCF with a silica solid core surrounded by a photonic crystal cladding with a triangular lattice of air- holes, this type guide light through a form of total internal reflection (TIR), called modified total internal reflection (MTIR).The guiding mechanism is defined as (modified) because the cladding refractive index is not a constant value, as in standard optical fibers, but it changes significantly with the wavelength, and the refractive index of the cladding can be varied by changing the hole pitch and the hole diameter . This offers a number of unique properties that cannot be achieved in conventional fibers. For example, the effective value (normalized frequency) is saturated against, where is the wavelength, resulting in single-mode operation over an ultrawide bandwidth (Poli, Cucinotta, and Selleri, 2007, Hirooka and Nakazawa, 2004). This mechanism is shown in figure (2.4).
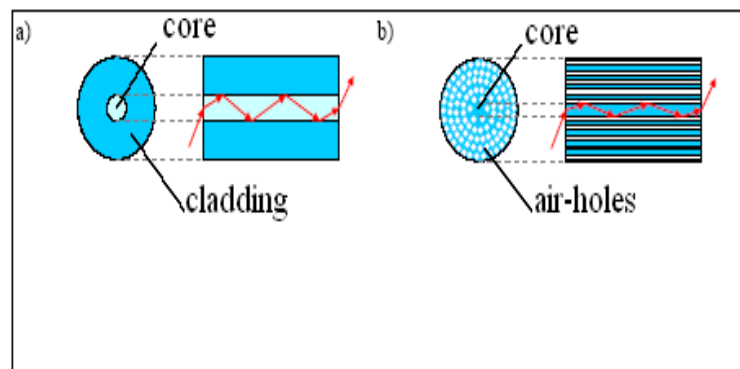

Figure (2.4): light guided by: (a) total internal reflection in conventional fiber (b) modified total internal reflection in photonic crystal fiber (Al Falah, 2009).

In a solid-core PCF, the pattern of air holes acts like a model sieve. In Figure (2.5 a), the fundamental mode is unable to escape because it cannot fit in the gaps between the air holes, (Al Falah, 2009), the air holes blocking the zero-order mode whose transverse effective wavelength (the component

perpendicular to the direction of propagation is too large to escape between the holes (Russell, 2003). whilst the higher order modes are able to leak away because their transverse effective wavelength is smaller (Antonpoulos, G. et al. 2006). This is shown in figure (2.5 b, c), that is why it is called modified total internal reflection (Babu, S. G. et al. 2005). If the diameter of the air holes is increased, the gaps between them shrink and more and more higher order modes become trapped in the sieve (Babu, S. G. et al. 2005).
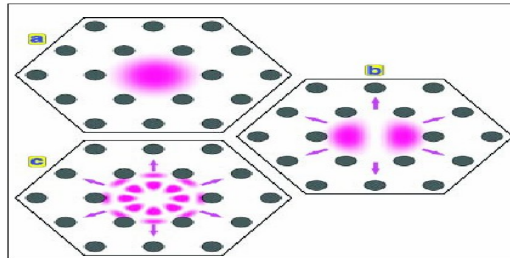

Figure (2.5): the pattern of air – holes acts like a model sieve (a) zero-order mode cannot squeeze between air holes (b) and (c)) higher-order modes can escape in the cladding(Russell, 2003) .

2.2.2 Photonic bandgap guidance (PBG)

One of the most interesting PCFs, with no counterpart in conventional fiber, when the PCF core region has a lower refractive index than the surrounding photonic crystal cladding (Ren, G. et al. 2007), light is guided by a mechanism different from total internal reflection that is, by exploiting the presence of the photonic bandgap (PBG) (Poli, Cucinotta, and Selleri, 2007, Roberts et al. 2006, Benabid, F. 2006). A photonic band gap (PBG) crystal is a structure that could manipulate beams of light in the same way semiconductors control electric currents (Buczynski, 2004. The band structure of semiconductors is the outcome of the interactions between electrons and the periodic variations in potential created by the crystal lattice. By solving the Schrodinger's wave

equation for a periodic potential, electron energy states separated by forbidden bands are obtained. PBGs can be obtained in photonic crystals, where periodic variations in dielectric constant that is in refractive index substitute variations in electric potential, as well as the classical wave equation for the magnetic field replaces the Schrodinger's equation. In a PBG fiber, periodic holes act as core and an introduced defect (an extra air hole) act as cladding. Since light cannot propagate in the cladding due to the photonic bandgap, they get confined to the core, even if it has a lower refractive index. PBG formation can be regarded as the synergetic interplay between two distinct resonance scattering mechanisms. The first is the "macroscopic" Bragg resonance from a periodic array of scatterers. This leads to electromagnetic stop gaps when the wave propagates in the direction of periodic modulation when an integer number, m=1, 2, 3…, of half wavelengths coincides with the lattice spacing, L, of the dielectric microstructure. The second is a "microscopic" scattering resonance from a single unit cell of the material. In the illustration, this (maximum backscattering) occurs when precisely one quarter of the wavelength coincides with the diameter, 2a, of a single dielectric well of refractive index n. PBG formation is enhanced by choosing the materials parameters a, L, and n such that both the macroscopic and microscopic resonances occur at the same frequency.

2.3 Guiding characteristics

The guiding characteristics of conventional fibers and the photonic crystal fibers are presented in the form of propagation diagram figure (2.6), whose

axes are the dimensionless quantities $\beta \Lambda$ and $\frac{\omega \Lambda}{C}$, where Λ is the inter

7

hole spacing and c is the speed of light in vacuum, This diagram indicates the ranges of frequency and axial wave vector component β where the light is evanescent (unable to propagate) (Russell, 2003).
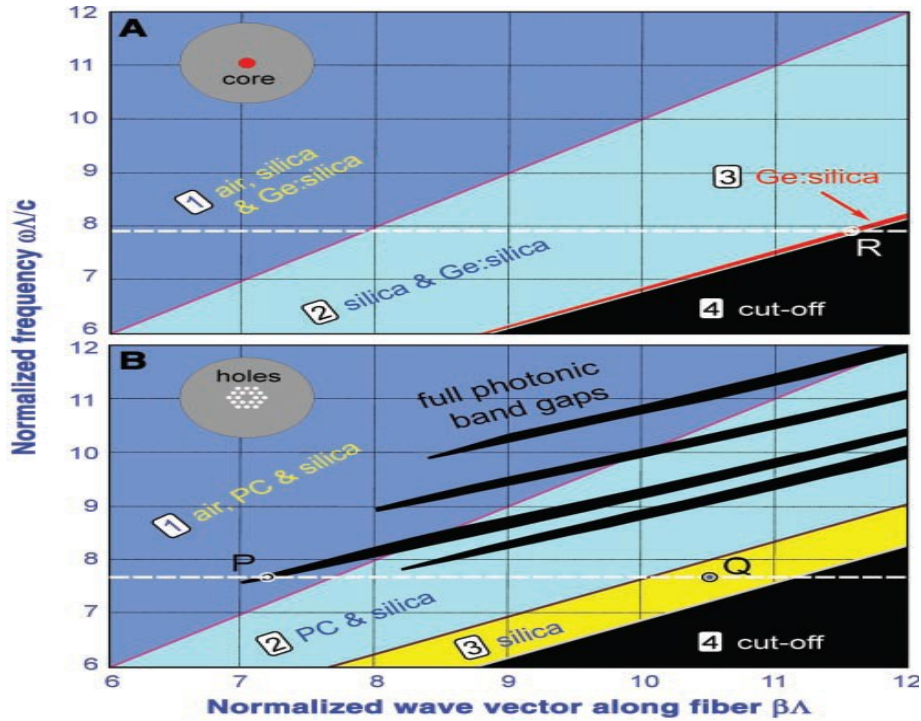

Figure (2.6): Propagation diagram of: (A) a conventional single-mode fiber, (B) Propagation diagram for a triangular lattice of air holes in silica glass (Russell, 2003)

At fixed optical frequency, the maximum possible value of β is set by

$$kn = \frac{\omega n}{C}$$, where n is the refractive index of the region under consideration.

For $\beta < kn$, light is free to propagate; for $\beta > kn$, it is evanescent. For conventional fiber (core and cladding refractive indices n_1 and, n_2 respectively), guided modes appear when light is free to propagate in the

doped core but is evanescent in the cladding (Fig. 2.6A) shows the propagation diagram for conventional single mode fiber (the schematic is in the top left-hand corner of the figure) with a germanium (Ge) doped silica core and a pure silica cladding. The guided modes at points like R, where light is free to propagate in the doped core, but is evanescent in the cladding (because total internal reflection operates there). The narrow red strip is where the whole of optical communications operates.

The same diagram for PCF is sometimes known as a band-edge or (finger) plot as shown in (Fig 2.6B). In a triangular lattice of circular air holes with an air filling fraction of 45%, light is free to propagate in every region of the fiber [air, photonic crystal (PC), and silica], this is shown in region (1) of the same figure. In region (2) propagation is turned off in the air but not in the PC and silica, and in (3), it is turned off in the air and the PC. In region (4), light is evanescent in every region. The black fingers represent the regions where full two-dimensional photonic band gaps exist, some of these fingers extend into $\beta < k$ where light is free to propagate in vacuum (Philip, R. 2001). Guided modes of a solid core PCF form at points such as Q, where light is free to travel in the core but unable to penetrate the PC. At point P, light is free to propagate in air but blocked from penetrating the cladding by the PBG, these are the conditions required for a hollow-core mode (Philip, R. 2001, Cregan, F. R. et al. 1999). This result indicates the hollow-core guidance is indeed possible in the silica-air systems. It is thought-provoking that the entire optical telecommunications revolution happened within the narrow strip $k n_2 \Lambda < \beta \Lambda < k n_1 \Lambda$ in fig 2.6 A (Roberts et al. 2006). The rich variety of new

features on the diagram for PCF explains in part why microstructuring extends the possibilities of fibers so greatly (Russell, 2003).

2.4 Fabrication procedure

The manufacturing of the conventional optical fibers involves two stages. In the first stage the preform with desired refractive index profile and the relative core – cladding dimensions is made by using a vapor deposition method. A typical preform is 1 m with a 20 mm diameter. In the second stage, the preform is drawn into a fiber using a precision-feed mechanism that feeds it into a furnace at a proper speed.

During this process, the relative core-cladding dimensions are preserved. Both stages preform fabrication and fiber drawing; involve sophisticated technology to ensure the uniformity of the core size and the index profile. For making the preform there are several alternative ways. There are three commonly used methods, Outside Vapor Deposition (OVD), Modified Chemical Vapor Deposition (MCVD) and Vapor phase Axial Deposition (VAD) (Agrawal, 2007, Agrawal, G., 2001, Mitschke, F. 2009).

In the drawing process in conventional fibers the viscosity is the only important parameter, but in the case of the PCFs there are several important parameters such as viscosity, gravity and surface tension. The choice of the base material strongly influences the technological issues and applications in the PCF fabrication process. By using the stack and drawing technique which introduced by Birks et al in 1996 to fabricate PCF a preform with the interest

structure but on a macroscopic scale firstly is create, it is possible to drilling several tens to hundred of holes in periodic arrangement into on final preform. The PCF preform is realized by stacking by hand a number of capillary silica tubes and rods to form the desired air–silica structure as shown in figure (2.7). This realizing preform allows the high flexibility design, since the core size and shape as well as the index profile throughout the cladding region can be controlled, then the capillaries and rods held together by thin wires and fused together during an intermediate drawing process into preform canes. Then the preform is drawn down on a conventional fibers drawing tower, greatly extending it is length, while reducing it is cross section from a few mm's to a few µm's (Poli, Cucinotta, and Selleri, 2007).
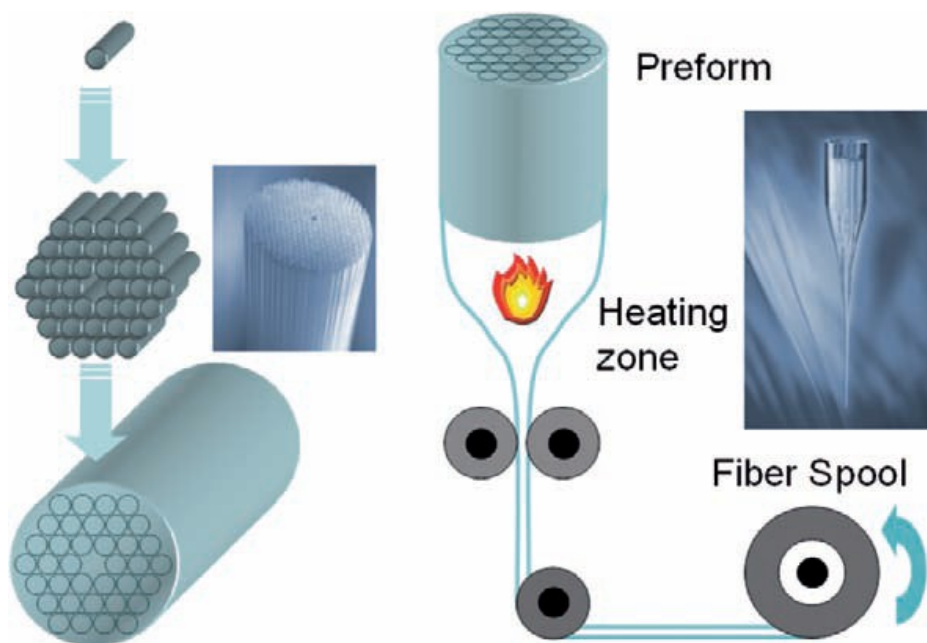

Figure (2.7): Scheme of the PCF fabrication process (Poli, Cucinotta, and Selleri, 2007).

The fabrication of a HC- PCFs, independently of their cladding structure, follows common core-procedure. It is based on drawing a tube (usually made

of silica) with a chosen wall thickness to hundreds of approximately 1 m long and approximately 1 mm diameter capillaries.then stacked by hand to the desired structure (stack). The stack is then fused and drawn to approximately 1 m long and a few millimeters diameter (canes). Finally, each cane is fused and drawn into a fiber (Benabid, F. 2006) . As shown in figure (2.8).
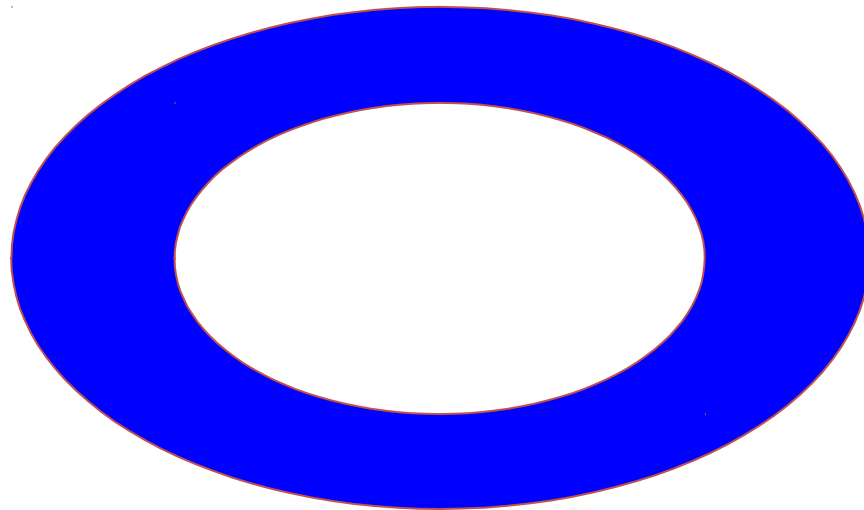

Figure (2.8): Schematic of the fabrication procedure of HC-PCFs (Benabid, F. 2006).

2.5 PCF Design Geometry properties

PCFs designed with different air – hole pattern have many properties which dependent on the design details some of them are (Mogilevtsev, Birks and Russell, 1998, Knight et al 1998, Nielse, Folkenberg and Mortensen, 2003 Nielsen et al. 2004).

 1. Endlessly single-mode guidance over very wide wavelength regions.

 2. Extremely small or extremely large mode areas than a conventional fiber, leading to very strong or weak optical nonlinearities

3. Low sensitivity to bend losses even for large mode areas.

4. The possibility to fill gases or liquids into the holes and make extremely strong birefringence for polarization-maintaining fibers.

5. The feasibility of multi-core designs, e.g. with a regular pattern of core structures in a single fiber, where there are some coupling between the cores.

6. Very unusual and engineerable chromatic dispersion properties, e.g. anomalous dispersion in the visible wavelength region.

We discuss the first two properties above in short details in the sub subsections.

2.5.1 Endlessly single mode fibers

PCF can be designed so that they are single mode for a large range of the spectrum, in other words the PFC designed to be endlessly single mode (no higher modes are supported regardless of the wave length). In conventional Single Mode Fiber (SMF) for the both types step index or graded index there are always a cut − off frequency above which the fibers starts to be multimode (Mortensen et al 2003). The V parameter plays a central role in the description of the number of guided modes in SMFs. V is defined as (Mortensen et al 2003):

$$V(\lambda) = \frac{2\pi}{\lambda} a \sqrt{n_1^2 - n_2^2}$$

(2. 1)

Where: a is the core radius, n_1 and n_2 are refractive indexes of the core and the cladding respectively.

In the convention fibers the cladding refractive index is wavelength independent and the V parameter is inverse dependence on the wavelength

(λ) for this relation the V parameter is often referred to as normalized frequency (Nielsen et al 2003).

The V parameter for PCF is given by (Lin C. and Stolen 1976):

$$V(\lambda)=\frac{2\pi}{\lambda}\Lambda\sqrt{n_1^2(\lambda)-n_2^2(\lambda)}$$
(2. 2)

Where: $n_c(\lambda)=\frac{C\beta}{\omega}$: core refractive index associate with effective index of the fundamental modes and $n_c(\lambda)$ is the effective index of the fundamental space – filling mode.
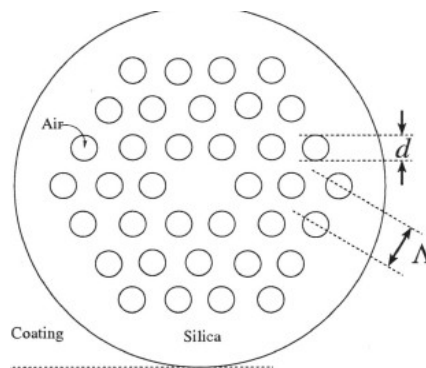
Figure (2.9): illustrated the air hole diameter (d) and the air- hole pitch (Λ)
(Lin C. and Stolen 1976)

For PCF a value of the effective refractive index of photonic cladding depends strongly on wavelength, while in conventional fibers it was almost constant.

The normalized frequency tends to a stationary value for short wavelengths. A refractive index of photonic cladding and therefore stationary value of normalized frequency is defined by the cladding structure, namely by the fill factor (the ratio of the hole diameter d to the period of the lattice $\Lambda \dot{c}$. Any

PCF fulfill this condition is usually called endlessly single mode. The cut - off normalized frequency for PCF estimated as 2.5 (Buczynski, 2004).

2.5.2 Large mode area

In single mode regime the conventional fibers have a strong limit on the core size and numerical aperture (NA). There is a maximum numerical aperture for any wavelength and core diameter makes the operation in single mode regime is possible. The difference between the core and the cladding refractive index is used to control the NA value. The mode field diameter (MFD) is limits by fabrication the conventional fiber with large mode area using appropriate method such as chemical vapor deposition (CVD).

In photonic crystal fiber the mode field diameter can vary in a single mode regime, depending on requirements. Large mode areas can be engineered by increasing the lattice pitch of the photonic cladding, decreasing the air hole diameter or increasing the size of the defect in photonic cladding (removal of more than one of the central air holes) (Buczynski, 2004).

2.6 Applications of PCF

The PCFs unique properties make it very attractive for a wide range of application like (Vokovic, N. 2010).

1. Fiber lasers and amplifiers, including high-power devices, mode-locked fiber lasers, etc.

2. Nonlinear devices such as suppercontinum generation (frequency combs), Raman conversion, parametric amplification, or pulse compression is possible by using PCF because both weak and strong nonlinearity can be achieved in PCF by proper design.

3. Telecom components, such as dispersion controller, filter and all optical switches.

4. Fiber-optic sensors.

5. Application in quantum optics such as generation of correlated photon pairs, electromagnetically induced transparency, etc.

2.7 pulse propagation in PCFs

All electromagnetic effects are governed by the four Maxwell equations in PCFs which is dielectric medium (no free charges or currents are present in the entre domain) is (Agrawal, 2007):

$$\nabla \times E = \frac{-\partial B}{\partial t} \tag{2.3}$$

$$\nabla \times H = \frac{\partial D}{\partial t} \tag{2.4}$$

$$\nabla . B = 0 \tag{2.5}$$

$$\nabla . D = 0 \tag{2.6}$$

Where E and H are the electric and magnetic fields respectively, both fields are functions is space and time, B and D the magnetic induction field and electric displacement. For a nonmagnetic isotropic medium such as PCFs, the flux densities B and D are related to E and H by the equations (Agrawal, 2007):

$$D = \varepsilon_0 E + P \tag{2.7}$$

$$B = \mu_0 H \tag{2.8}$$

Where: ε_0 is vacuum permittivity, μ_0 is vacuum permeability and P is the induced electric polarization (Reichenbach 2007).

By applying the operator curl on the equation (2.3) and using equations (2.4), (2.7) and (2.8) into the result, we obtained the wave equation that describes the pulse propagation in PCFs as (Agrawal, 2007):

$$\nabla \times \nabla \times E = \frac{1}{C^2} \frac{\partial^2 E}{\partial t^2} - \mu_0 \frac{\partial^2 P}{\partial t^2}$$
(2.9)

Where the induced electric polarization P is related to the electric field $E(r,t)$ (far from medium resonance) is given by:

$$P = \varepsilon_0 \left(\chi^1 \cdot E + \chi^2 : EE + \chi^3 \vdots EEE + \ldots \right)$$
(2.10)

The electric field $E(r,t)$ can be expressed in terms of slowly varying envelope approximation as:

$$E(r,t) = \frac{1}{2} \hat{x} [E(r,t) \exp(i\omega_0 t) + c.c.]$$
(2.11)

Where $E(r,t)$ is a slowly varying complex envelope, $\hat{x}$ is the polarization unit vector, $c.c.$ stands for complex conjugate and ω_0 is an angular optical frequency.

By using Fourier analysis the wave equation (2.9) in frequency domain becomes:

$$\nabla^2 \tilde{E} + \varepsilon(\omega) \tilde{E} k_0^2 = 0$$
(2.12)

Where k_0 free space wave number is defined as:

$$k_0 = \frac{\omega}{C} = \frac{2\pi}{\lambda}$$
(2.13)

And $\varepsilon(\omega)$ is frequency dependent dielectric constant is expressed as:

$$\varepsilon(\omega) = 1 + \tilde{\chi}^{(1)}(\omega) + \varepsilon_{NL} \tag{2.14}$$

Where ε_{NL} the nonlinear contribution of dielectric constant is treated as constant during the pulse propagation and defined as:

$$\varepsilon_{NL} = \frac{3}{4} \chi^{(3)}_{xxxx} |E(r,t)|^2 \tag{2.15}$$

And $\tilde{\chi}^{(1)}(\omega)$ is Fourier transform of $\chi^{(1)}(t)$. It is real and imaginary parts are related to the refractive index $\tilde{n}(\omega)$ and the attenuation coefficient $\alpha(\omega)$ by the equation:

$$\varepsilon = \left(\tilde{n} + \frac{i\alpha c}{2\omega} \right)^2 \tag{2.16}$$

$\tilde{n}(\omega)$ is given by:

$$\tilde{n}(\omega, |E|^2) = n(\omega) + n_2 |E|^2 \tag{2.17}$$

Then the following equations are obtained from equations 2.16 and 2.17 $n(\omega)$ and $\alpha(\omega)$ are related to $\chi^{(1)}$ by the relations:

$$n(\omega) = 1 + \frac{1}{2} \Re[\tilde{\chi}^{(1)}(\omega)] \tag{2.18}$$

$$\alpha(\omega) = \frac{\omega}{nC} \Im[\tilde{\chi}^{(1)}(\omega)] \tag{2.19}$$

Where $\Re$ and $\Im$ are real and imaginary parts. Due to low losses in fiber the imaginary part of $\varepsilon(\omega)$ is negligible in comparison to the real part, then the $\varepsilon(\omega)$ can be replaced by $\tilde{n}^2(\omega)$ so that equation 2.12 becomes:

18

$$\nabla^2 \tilde{E} + \tilde{n}^2(\omega) \tilde{E} k_0^2 = 0 \qquad (2.20)$$

$\tilde{E}$ is defined as:

$$\tilde{E}(r,\omega) = \int_{-\infty}^{\infty} \dot{\iota} \quad \begin{array}{c} iwtdt \\ E(r,t) \exp \dot{\iota} \end{array} \qquad (2.21)$$

By using the method of separation variables for solution the optical field, the envelope is in a form:

$$E(r,t) = F(x,y) A(z,t) \exp(i\beta_0 z) \qquad (2.22)$$

Where $F(x,y)$ is transverse mode distribution, $A(z,t)$ is slowly varying

function of z and $\beta_0 = \beta(\omega_0)$ is the wave number at carrier frequency

(Agrawal, 2007).

In order to be able to observe different nonlinear effects in PCFs, the solution

of equation (2.20) can be assumed as the following form:

$$\tilde{E}(r,\omega-\omega_0) = F(x,y)\tilde{A}(z,\omega-\omega_0)\exp \dot{\iota} \quad \begin{array}{c} i\beta_0 z \end{array} \qquad (2.23)$$

Where $\tilde{A}(z,\omega)$ is slowly varying function of z, β_0 is the wave number and

$F(x,y)$ corresponds to the modal distribution in the fiber. Equation 1.30

leads to the following two equations for $F(x,y)$ and $\tilde{A}(z,\omega)$:

$$\frac{\partial^2 F}{\partial x^2} + \frac{\partial^2 F}{\partial y^2} + \left[\varepsilon(\omega)k_0^2 - \tilde{\beta}^2\right]F = 0 \qquad (2.24)$$

$$2i\beta_0 \frac{\partial \tilde{A}}{\partial z} + \left(\tilde{\beta}^2 - \beta_0^2\right)\tilde{A} = 0 \qquad (2.25)$$

Where the second order derivative $\frac{\partial^2 \tilde{A}}{\partial z^2}$ is ignored, since $\tilde{A}(z,\omega)$ is

assumed to be slowly varying function of z. the eigenvalu $\tilde{\beta}$ can be written

by $\tilde{\beta}(\omega)=\beta(\omega)+\Delta\beta$

Where:

$$\Delta\beta=k_0\frac{\displaystyle\iint_{-\infty}^{\infty}\Delta n|F(x,y)|^2 dxdy}{\displaystyle\iint_{-\infty}^{\infty}|F(x,y)|^2} \qquad (2.26)$$

Where: $x \wedge y$ are the transverse coordinates.

Equation (2.25) can be approximate by replacing $(\tilde{\beta}^2-\beta_0{}^2)$ with

$2\beta_0(\tilde{\beta}-\beta_0)$ as:

$$\frac{\partial \tilde{A}}{\partial z}-i[\beta(\omega)+\Delta\beta-\beta_0]\tilde{A}=0 \qquad (2.27)$$

By transforming the equation above back to time domain, the propagation

equation of A(z,t) can be obtained. However, as an exact functional form of

$\beta(\omega)$ is rarely known, note that $\beta(\omega)$ can be expand in Tyler series about

the center frequency (ω_0) as:

$$\beta(\omega)=\beta_0+(\omega-\omega_0)\beta_1+\frac{1}{2}(\omega-\omega_0)^2\beta_2+\frac{1}{6}(\omega-\omega_0)^3\beta_3+\dot\iota \qquad (2.28)$$

Where β_m is mth order dispersion coefficient defined as:

$$\beta_m = \left(\frac{d^m\beta}{d\omega^m}\right)\omega = \omega_0 \qquad m = 1, 2, 3, \ldots$$

By substituted equation 2.27 in 2.28 and after taking the inverse Fourier transform, during the transform $(\omega - \omega_0)$ is replaced by $i\left(\frac{\partial}{\partial t}\right)$ we get:

$$\frac{\partial A}{\partial z} = -\beta_1 \frac{\partial A}{\partial t} - \frac{i}{2}\beta_2 \frac{\partial^2 A}{\partial t^2} + \frac{1}{6}\beta_3 \frac{\partial^3 A}{\partial t^3} + \ldots + i\Delta\beta A \qquad (2.29)$$

Where $\Delta\beta$ is evaluated by using equations 2.20 and 2.25, so that the following equation is defined:

$$\frac{\partial A}{\partial z} + \beta_1 \frac{\partial A}{\partial t} + \frac{i}{2}\beta_2 \frac{\partial^2 A}{\partial t^2} - \frac{1}{6}\beta_2 \frac{\partial^3 A}{\partial t^3} + \ldots + \frac{\alpha}{2}A = i\gamma |A|^2 A \qquad (2.30)$$

Equation2.30 is called the nonlinear Schrodinger equation (NLSE) describes the pulse propagation in optical fiber. Its includes the effect of the fiber losses through the parameter α, the effect of fiber nonlinearity through γ coefficient and fiber dispersion through β_m .

The nonlinearity coefficient γ is given by:

$$\gamma = \frac{n_2 \omega \int\limits_{-\infty}^{\infty}\int\limits_{-\infty}^{\infty} |F(x,y)|^4 dxdy}{c\left(\int\limits_{-\infty}^{\infty}\int\limits_{-\infty}^{\infty} |F(x,y)|^2 dxdy\right)^2} \qquad (2.31)$$

Equation 2.49 is equivalent to:

$$\gamma = \frac{2\pi n_2}{\lambda A_{eff}} \qquad (2.32)$$

Where A_{eff} is the effective area, introduced to estimate the optical field concentration inside the fiber and defined as:

$$A_{eff} = \frac{\left(\int\limits_{-\infty}^{\infty}\int\limits_{-\infty}^{\infty}|F(x,y)|^2 dxdy\right)^2}{\int\limits_{-\infty}^{\infty}\int\limits_{-\infty}^{\infty}|F(x,y)|^4 dxdy} \qquad (2.33)$$

2.8 Different propagation regimes

The nonlinear Schrödinger equation governs propagation of optical pulse inside PCFs. For pulse width greater than 5 picoseconds the NLSE becomes (Agrawal, 2007):

$$i\frac{\partial A}{\partial z} = \frac{-i\alpha}{2}A + \frac{1}{2}\beta_2\frac{\partial^2 A}{\partial T^2} - \gamma|A|^2 A \qquad (2.34)$$

Where A is the slowly varying amplitude of the pulse envelope and T is measured in a frame of reference moving with the pulse at the group velocity

$$v_g \quad (\quad T = t - \frac{z}{v_g} ¿$$

Equation (1.43) the terms in left hand side represent respectively, the effects of fiber losses, dispersion and nonlinearity of pulse propagation inside fibers. Depending on the initial width T_0 and the peak power P_0 of the incident pulse, either dispersive or nonlinear effect may dominate along the fiber. Two length scales overs which the dispersion or nonlinearity effects become important for pulse propagation, known as the dispersion length L_D (

$L_D = \dfrac{T_0^2}{|\beta_2|}$) and nonlinear length L_{NL} ($L_{NL} = \dfrac{1}{\gamma P_0}$), where γ is

nonlinearity coefficient and β_2 is Group velocity dispersion (GVD).

By introduce a time scale normalized to the input pulse width T_0 as:

$$\tau = \frac{T}{T_0} = \frac{t - \dfrac{z}{v_g}}{T_0} \tag{2.35}$$

At the same time, we introduce a normalized amplitude U as:

$$A(z,\tau,) = \sqrt{P_0} \exp\left(\frac{-\alpha z}{2}\right) U(z,\tau) \tag{2.36}$$

Where: P_0 is the peak power of the incident pulse, the fiber losses can

appear by the exponential in the equation. By using Equations 2.34 and 2.36

$U(z,\tau)$ is found to satisfy:

$$i \frac{\partial U}{\partial z} = \frac{sgn(\beta_2)}{2 L_D} \frac{\partial^2 U}{\partial \tau^2} - \frac{\exp(-\alpha z)}{L_{NL}} |U|^2 U \tag{2.37}$$

Where $sgn(\beta_2)$ = +1 when $\beta_0 > 0$ and $sgn(\beta_2)$ = -1 when $\beta_0 < 0$

Depending on the relative magnitudes of L , L_D , L_{NL} , the propagation

behavior can be classified in four categories.

When fiber length is such that $\ll L_{NL} \wedge L \ll L_D$, neither dispersive nor

nonlinear effects dominate, pulse evolution and pulse propagates maintaining

it is shape during the propagation. As pulses becomes shorter and more

intense. If the fiber length is such that $L \ll L_{NL} \wedge L ~ L_D$ the pulse evolution is

23

then governed by GVD and the nonlinear effects is minority. The dispersion dominant regime is applicable whenever:

$$\frac{L_D}{L_{NL}} = \frac{\gamma P_0 T_0^2}{|\beta_2|} \ll 1$$

(2.38)

When the fiber length is such that $L \ll L_D \wedge L \; L_{NL}$ the pulse evolution is governed by SPM that produce change in the pulse spectrum, the nonlinearity dominant regime is applicable whenever:

$$\frac{L_D}{L_{NL}} = \frac{\gamma P_0 T_0^2}{|\beta_2|} \gg 1$$

(2.39)

When fiber length L is longer or comparable to both L_D and L_{NL}, dispersion and nonlinearity act together as the pulse propagates along the fiber, these interplay of dispersion and nonlinearity effects can lead to a qualitatively different behavior compared with that expected from GVD or SPM alone(Agrawal, 2007).

For ultrashort optical pulse higher order nonlinear effects are included in account then the normalized Schrödinger equation write as:

$$|U|$$
$$(¿¿2U) - \tau_R U \frac{\partial |U|^2}{\partial \tau}$$
$$|U|^2 U + is \frac{\partial}{\partial \tau} ¿ \qquad (2.40)$$
$$\frac{\partial U}{\partial z} + i \frac{sgn(\beta_2)}{2 L_D} \frac{\partial^2 U}{\partial \tau^2} = \frac{sgn(\beta_3)}{6 \dot{L}_D} \frac{\partial^3 U}{\partial \tau^3} + i \frac{e^{-\alpha z}}{L_{NL}} ¿$$

Where $\dot{L}_D$ is defined as:

$$\dot{L}_D = \frac{T_0^3}{|\beta_3|}$$

The parameter s and τ_R govern the effect of self – steeping and intrapulse Raman scattering and are expressed as:

$$s = \frac{1}{\omega_0 T_0} \quad , \qquad\qquad \tau_R = \frac{T_R}{T_0}$$

(2.41)

2.9 literature review

The amplification of femtosecond laser has been experimentally investigated around 1.060 μ m wavelength through an optical fiber based on stimulated Raman scattering (SRS)the results showed that the self phase modulation (SPM) leads to compress the laser spectral width from 6.96 nm to 5 nm with small effect on the maximum nonlinear phase shift (Kbashi, J. H. et al 2009). The self phase modulation leads to broaden the spectral width from 5nm to 38nm after simulated picoseconds pulse propagation in monomode optical fiber (Kbashi and Abdl Daim 2012). Femtosecond laser pulse propagation in monomode optical fibers is demonstrated and investigated numerically (by simulations) and experimentally the results showed that self phase modulation (SPM) leads to compression of the spectral width from 5 nm to 2.1nm after propagation of different optical powers in fibers of different length The varying optical powers produced a varying phase shift. The output spectral width also

changed with the fiber length at a given peak power (Kbashi, J. H. et al. 2010). Quantum dot nanocoatings have been deposited by means of the Layer-by-Layer technique on the inner holes of Photonic Crystal Fibers (PCFs) for the fabrication of temperature sensors. The optical properties of these sensors including absorbance, intensity emission, wavelength of the emission band, and the full width at half maximum (FWHM) have been experimentally studied for a temperature range from -40^0 to 70^0C. Omnichrome laser tuned at 470 nm was used in this experiment. The results showed that the maximum peak of the laser curve was changes with the temperature. Also the wavelength and the width of this peak are increased as far as the temperature rises (Larrion, B. et al. 2009). Cross phase modulation (XPM) and induced focusing due to optical nonlinearities in optical fibers and bulk materials. The results showed that the XPM causes pulse spectra to broaden more than with the Self phase modulation (SPM), when the spectrum of 527 nm with 80 μJ picoseconds pass in BK7 glass at 9 cm length is used (Nielse, Folkenberg and Mortensen, 2003). Self Phase Modulation and Spectral Broadening of Optical Pulses in Semiconductor Laser Amplifiers, was studied theoretically and experimentally. The results related to the amplification of short optical pulses in semiconductor amplifiers. The SPM lead to broadening the spectral as a result of gain saturation that is responsible for time dependent variations in carrier density (Mogilevtsev, Birks and Russell, 1998). Generation of supercontinum light in PC fiber is studied. When the fs or ps laser pulses interacts with nonlinear medium can generate new frequencies which lead to broaden the pulse spectrum, according to Self phase modulation, four waves maxing and Stimulated Raman scattering (Knight et al 1998).